Quantum Electronics **51** (12) 1090–1095 (2021)

https://doi.org/10.1070/QEL17657

Study of the output beam spatial characteristics of a cascade Raman laser with multimode diode pumping

A.G. Kuznetsov, S.I. Kablukov, E.V. Podivilov, S.A. Babin

Abstract. **We report a study of the spatial characteristics of the beam output from a multimode-pumped SRS cascade laser. The intensity profiles of transmitted pump radiation beams, as well as of the first and second orders Stokes SRS generation, is measured in two different laser configurations: in a classical laser with two pairs of reflectors and in a scheme with a half-open cavity for the second order Stokes component. The dynamics of changes in the intensity profiles of the radiation beams in the two considered resonators is shown to differ significantly. The data obtained for the beam profiles are analysed together with the power characteristics of the cascade Raman laser within the framework of a balance model of interaction between pump radiation and the Stokes components of the SRS.**

Keywords: *Raman lasing, multimode gradient fibre, fibre Bragg gratings, balance model.*

1. Introduction

Recently, Raman lasers based on a graded-index fibre (GIF) have attracted much attention due to the possibility of efficient conversion of multimode ($M^2 \approx 30$) radiation of high-power laser diodes (LDs) into a Stokes beam with good quality ($M^2 \approx 2-3$) in an all-fibre resonator with fibre Bragg gratings (FBGs) and fibre combiners of pump radiation from several LDs [1, 2]. Such Raman lasers using commercially available GIFs and LDs with a wavelength of 915–960 nm can generate Stokes radiation in the wavelength range of less than 1 μm, where efficient and stable operation of fibre lasers based on Yb-doped single-mode fibres is difficult due to photodarkening of the fibre and other interfering effects [3]. Connecting several (up to three) high-power LDs to GIFs with a core 100 μm in diameter using a multimode pump combiner makes it possible to increase the total pump power at the fibre input to ~200 W and generate Stokes radiation with a power of 50–60 W at wavelengths of 954 nm [1] and 976 nm [4] using LDs with a centre wavelength of 915 and 940 nm, respectively. It is noteworthy that the generated SRS first order Stokes radiation has a better beam quality ($M^2 \approx 2$) compared to the quality of the pump beam from high-power multimode LDs ($M^2 \approx 30$).

The use of cascade multimode Raman lasers with generation of higher order Stokes components [5] makes it possible to further improve the beam quality, in particular, in Ref. [6], the beam quality of the generated second order Stokes SRS radiation ($\lambda = 1019$ nm) reached ~1.35, which is close to the diffraction limit. Despite the fact that the effect of 'SRS clean-up' of the beam in gradient index fibres is well known [7], the explanation given in the literature is qualitative and based on a complicated analysis of the overlap integrals of various transverse modes of pump and Stokes radiation beams [8]. To construct a more complete model of the interaction of pump and SRS waves, it is necessary to measure the output parameters of the beams directly in the plane of the output end of the laser. In Ref. [9], the intensity profiles of different spectral components of the output radiation of a single-stage SRS laser were recorded for the first time, the optical measurement scheme providing an image of the output fibre face. In this way, the intensity profiles of the pump and the first order Stokes SRS radiation waves were obtained, and the effect of 'hole burning' in the pump beam was discovered. The effect was qualitatively explained within the framework of the proposed balance model, in which the local interaction of the pump wave and the Stokes wave is assumed. Since the transverse size of the Stokes radiation beam is much smaller than that of the pump beam (due to the small transverse size of the output FBG that forms the resonator), a hole is burned out in the central region of the pump beam during effective SRS conversion. However, the balance model does not explain quantitatively the experimentally observed significant increase in the intensity of the Stokes wave as compared to the intensity of the pump radiation.

This paper continues the study of the interaction between pump and SRS waves. However, in contrast to previous studies, a cascaded scheme of a Raman laser with sequential generation of the first and second Stokes components is considered (a laser with two FBG pairs and a laser with a half-open second cavity, that is, with one FBG and Rayleigh feedback for the second Stokes component). The output profiles of the intensity of the pump radiation, as well as the radiation of the first and second order Stokes SRS components, were measured. A comparison of the changes in the intensity and output power profiles of different components for the two types of resonator is carried out, which shows their significant difference.

A.G. Kuznetsov, S.I. Kablukov Institute of Automation and Electrometry, Siberian Branch, Russian Academy of Sciences, prosp. Akad. Koptyuga 1, 630090 Novosibirsk, Russia;
e-mail: leks.kuznecov@gmail.com;
E.V. Podivilov, S.A. Babin Institute of Automation and Electrometry, Siberian Branch, Russian Academy of Sciences, prosp. Akad. Koptyuga 1, 630090 Novosibirsk, Russia; Novosibirsk State University, ul. Pirogova 2, 630090 Novosibirsk, Russia

Received 26 October 2021
Kvantovaya Elektronika **51** (12) 1090–1095 (2021)
Translated by V.L. Derbov

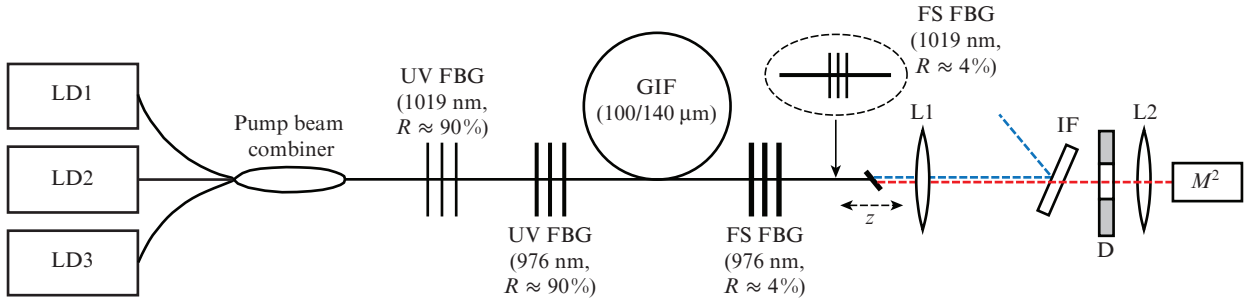

Figure 1. Schematic of a multimode Raman fibre laser: (LD1–LD3) multimode LDs; (UV FBG) high-reflective FBG inscribed using UV radiation; (FS FBG) low-reflective FBG inscribed using the point-by-point method with femtosecond pulses; (L1, L2) lenses; (IF) interference filter; (D) diaphragm.

2. Experiment

A schematic of a Raman fibre laser is shown in Fig. 1. The first stage of the laser was formed by a high-reflective FBG inscribed by the interferometric method [10] with UV laser radiation, having a reflection coefficient $R \approx 90\%$ at a Bragg wavelength of 976 nm and an output low-reflection FBG fabricated by the method of point-by-point writing by femtosecond pulses [11], with $R \approx 4\%$ at $\lambda = 976$ nm. The second stage was formed by a high-reflective FBG, reflecting at $\lambda = 1019$ nm (the second Stokes component of the SRS), and by random Rayleigh backscattering from the other side of the resonator, that is, the so-called half-open scheme of a laser cavity with random feedback (random Raman fibre laser, RRFL). We also studied a classic two-stage Raman laser (RFL), which was formed from the first scheme by adding a low-reflective output FBG for the second Stokes component ($R \approx 4\%, \lambda = 1019$ nm).

For pumping, three high-power (more than 100 W) multimode LDs with fibre outputs (step-index fibre, 105/125 μm, NA = 0.22) and a lasing wavelength of ~938 nm were used, which were connected to the corresponding inputs of the pump combiner 3 × 1. The output of the combiner was spliced to a fibre-optic line with a length of ~1 km with a gradient profile of the refractive index of the core (GIF, 100/140 μm) and a numerical aperture of 0.29. The pump combiner loss was about 2 dB. The end face of the laser output fibre was cleaved at an angle of 10°–15° to eliminate the influence of Fresnel reflection. The beam emerging from the fibre was collimated by lens L1. Focusing lens L2 is part of the beam quality meter (Thorlabs M^2-MS), forming a waist inside the device. To obtain the intensity profile in the plane of the fibre end face, the CCD array of the beam meter was installed at the focus of lens L2. The position of the output end of the laser was aligned with the main optical axis of collimating lens L1 in order to achieve the maximum depth of the dip in the pump radiation intensity profile, which occurs at the onset of generating the Stokes radiation.

To measure the transverse profiles of the intensity distribution of the radiation beams of the first and second Stokes orders and the transmitted pump radiation in the scheme shown in Fig. 1, we used three different interference filters IF with centre transmission wavelengths of 1025 nm ($\Delta\lambda$ = 50 nm), 976 nm ($\Delta\lambda = 25$ nm) and 950 nm ($\Delta\lambda = 25$ nm). Thus, the spectral component of interest to us was selected. Note that Ref. [9] also considered the possibility of recording the intensity distribution profile at the output of an optical fibre in a similar scheme and reported a deterioration in the contrast of the measured profile with a longitudinal deviation of the output fibre from the optimal position. For a qualitative assessment of the influence of higher transverse modes on the formed transverse profile of the intensity distribution, diaphragm D with a variable diameter was installed in the scheme.

3. Experimental results

Figure 2 shows the measured powers of the transmitted pump radiation, as well as the radiation of the first and second order Stokes SRS components for two laser configurations: RFL and RRFL. At a pump power up to 100 W at the input, the power of the transmitted pump radiation grows linearly with increasing pump power at the input, and the slope of this dependence is determined by the loss in the fibre line (~3 dB). At a pump power of ~110 W at the input, the generation of the first order Stokes SRS radiation ($\lambda = 976$ nm) begins, which depletes the pumping, changing, accordingly, the slope of the dependence of the transmitted pump radiation power on its input power. An important difference between the two resonator schemes for the second Stokes component (RFL and RRFL) is that the RRFL exhibits a decrease in the power

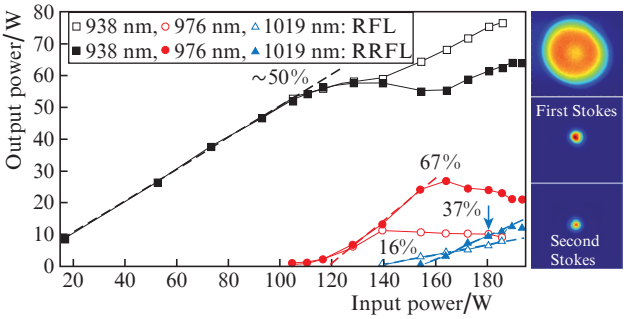

Figure 2. (Colour online) Measured powers of transmitted pump radiation ($\lambda = 938$ nm), first ($\lambda = 976$ nm) and second ($\lambda = 1019$ nm) order Stokes components of the SRS as functions of the input pump power, as well as the corresponding typical profiles of the intensity of radiation beams at a pump power above the second order Stokes SRS generation threshold (RRFL). The arrow indicates the threshold for the generation of the third order Stokes SRS component.

of the transmitted pump radiation due to its depletion during SRS conversion to first order Stokes radiation up to the beginning of generating the second order Stokes SRS. In the RFL, the threshold of the second order Stokes SRS is lower and the Stokes radiation of the first order begins to deplete earlier. This leads, in turn, to an almost linear dependence of the transmitted pump power on its input value with a break (change in the slope curve) in the range of input pump powers of 100–140 W. The quality parameter M^2 of the pump beam from three LDs at the laser input (after the pump combiner) was ~27. Due to the SRS cleaning effect and the selective properties of the FBG, the generated beam of first order

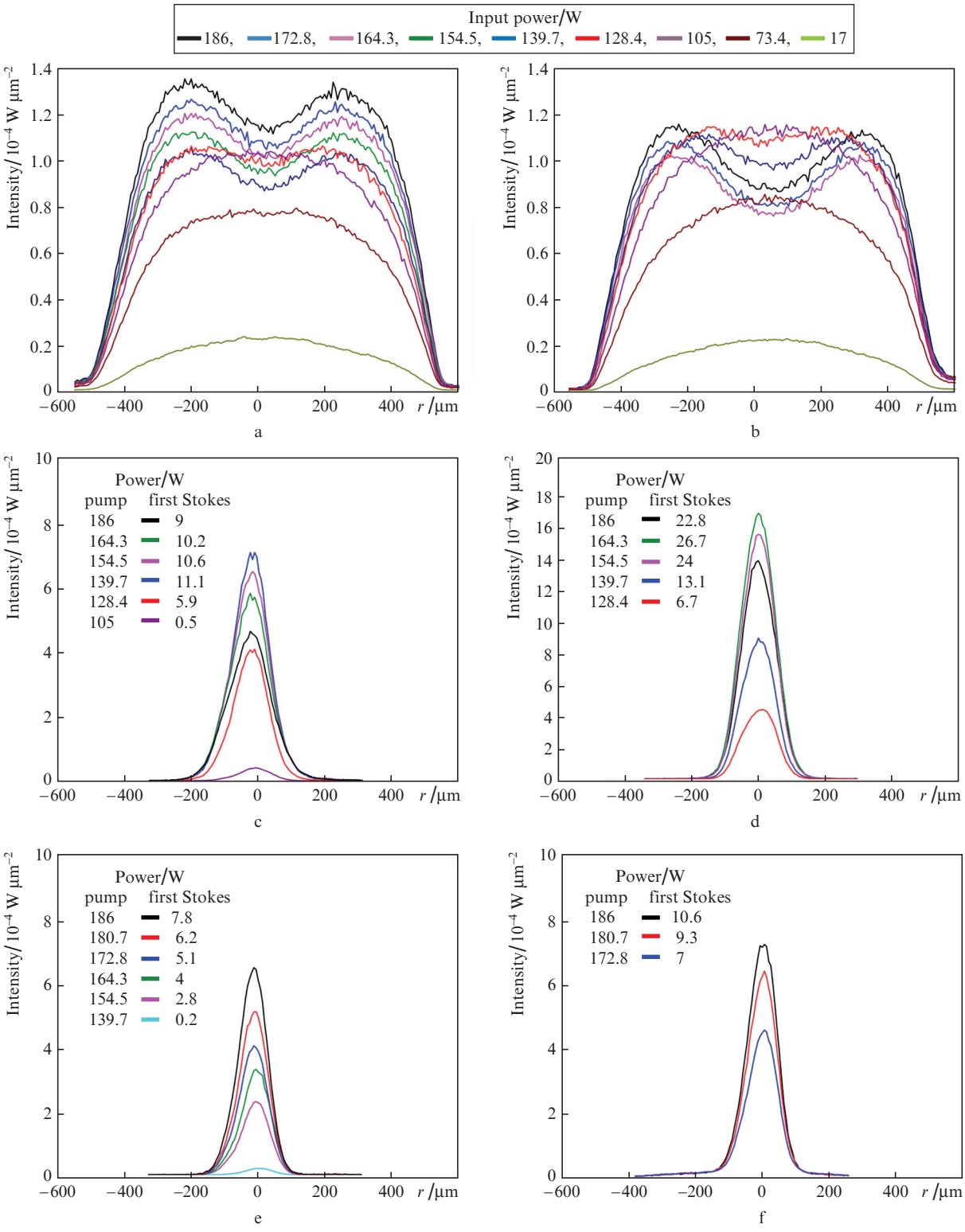

Figure 3. (Colour online) Transverse profiles of intensity distributions of transmitted pump radiation (a), first (c) and second order (e) Stokes components of SRS in the RFL scheme, as well as similar profiles (b, d, f) in the RRFL scheme at different input pump powers.

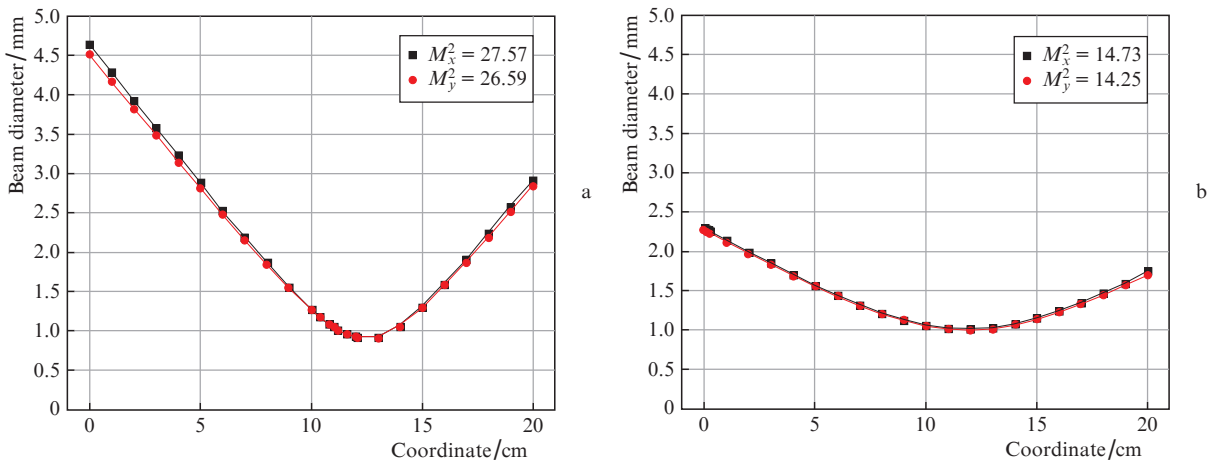

Figure 4. (Colour online) Results of measuring the quality of the transmitted pump radiation beam up to the SRS generation threshold with (a) open and (b) half-open diaphragms.

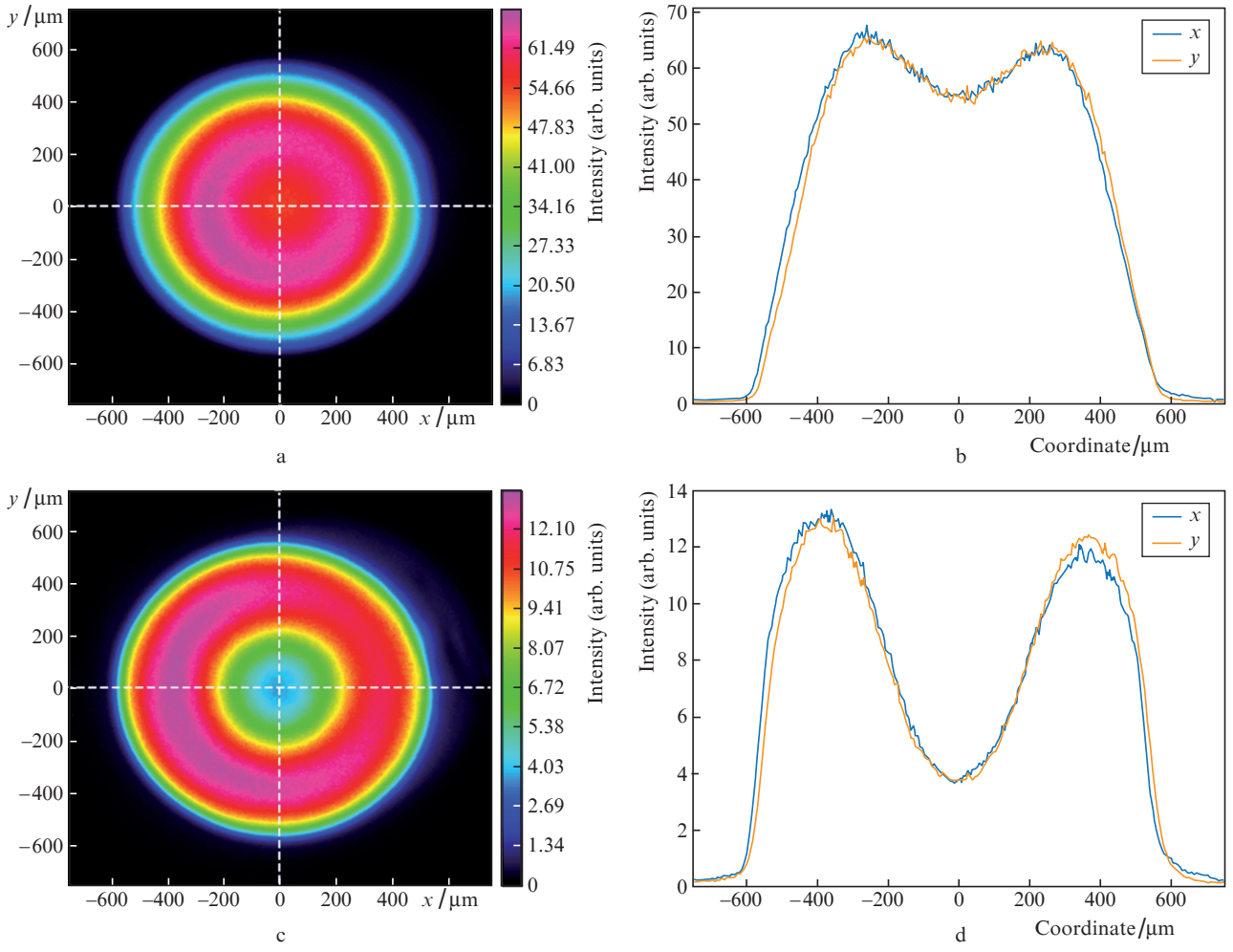

Figure 5. (Colour online) Intensity profiles of the transmitted pump radiation beam in the case of pumping above the generation threshold of the first Stokes SRS component with (a, b) open and (c, d) half-open diaphragm.

Stokes radiation has a quality parameter of 1.7–1.8, and the quality of the second order Stokes beam improves even more up to 1.3–1.4 for both resonator configurations [5]. Images of all three beams emerging from the laser with simultaneous generation of the first and second order Stokes components are shown in Fig. 2 on the right, where the resulting dip in the centre of the pump beam is visible.

Figure 3 shows the transverse profiles of the intensity distributions of the transmitted pump radiation, normalised to the readings of the power meter, as well as the first and second

Stokes orders of the SRS, depending on the pump power at the input for the RFL and RRFL schemes. Up to the SRS lasing threshold, the pump beam profile is close to parabolic (in accordance with the profile of the GIF refractive index). When a first order Stokes wave is generated, a dip is burned out in the pump profile, the width of which is much larger than the width of the Stokes beam profile, and when the second Stokes component is generated, the amplitude of the transmitted wave in the RFL case begins to grow again practically without changing the profile shape. A somewhat different situation is observed in the RRFL, where the value of the dip burnt in the pump profile during the generation of the first Stokes component is much larger in accordance with its higher power. In this case, the increase in the amplitude of the pump intensity profile begins with the onset of generation of the second Stokes component, as in the previous case, but this growth itself is small. Note also that the first order Stokes radiation beams in both configurations are practically not distorted upon the appearance of the second order Stokes generation and remain close in shape to the described Gaussian intensity distribution function.

For a qualitative assessment of the contribution of higher transverse modes to the dip in the transverse profile of the pumping radiation intensity distribution, a diaphragm (D, Fig. 1) was placed in front of the beam quality meter, which could be in two positions: completely open and overlapping half of the pump beam. Up to the SRS generation threshold, the quality M^2 of the pump beam after passing through a GIF with a length of 1 km is ~27 (Fig. 4a), while after blocking half of the beam with the diaphragm, it becomes equal to ~14.5 (Fig. 4b). Thus, the diaphragm is a selector that blocks high order transverse modes, the mode spots of which have a larger diameter compared to the lower order modes. Figure 5 shows the intensity profiles of the transmitted laser pump radiation (in the RFL configuration) in the case of generating the first Stokes component with open and half-open apertures. It can be seen that with a half-open aperture, the depth of the dip increases significantly. This suggests that the central region of the beam contains part of the energy of the Gauss–Laguerre modes, which neutralise the dip, which is obviously not taken into account in the balance model [9] and partially explains the significant discrepancy between the measurement and simulation results.

4. Discussion of the results and conclusions

Thus, the measurements have shown that, up to the SRS generation threshold, the transverse profile of the intensity distribution of the transmitted pump radiation ($M^2 \approx 27$) is close to parabolic. This corresponds to a uniform distribution of transverse modes achieved due to their possible mixing during propagation in a 1 km long gradient fibre wound on a coil. When an intense Stokes wave with a quality parameter $M^2 \approx 1.8$ is generated, a spatial hole is burned out in the transverse profile of the intensity distribution of the transmitted pump radiation, and the dip increases significantly with increasing Stokes radiation power up to the generation threshold of the second Stokes SRS component in the RRFL scheme. When the generation of this component begins, the amplitude of the entire profile of the pump radiation intensity begins to increase (without changing the shape). At the same time, in the RFL scheme, the formation of a dip is replaced rather quickly by an increase in the amplitude of the entire pump intensity profile, since the generation threshold of the second Stokes component of the SRS is much lower here and the power of the first Stokes component does not have time to increase significantly.

In contrast to the transverse profile of the intensity distribution of the transmitted pump radiation, the intensity profile of the first Stokes component of the SRS does not change its shape when depleted by the higher order SRS components and remains close to Gaussian. The width of the dip in the transverse profile of the intensity distribution of the transmitted pump radiation, as in Ref. [9], is noticeably larger than for the generated SRS beams, which is associated with the effect of mixing of transverse modes during the propagation of the pump wave along the fibre. At the same time, SRS Stokes beams 'do not spread' in transverse higher modes, presumably due to the effect of the Kerr self-cleaning of the beam [12]. Since the mode compositions of the first and second Stokes components of the SRS in the fibre are close and described by Gaussian distributions (close to single-mode), there is also no distortion of the intensity profiles during their interaction. The burning of a hole in the pump beam is again qualitatively described by the balance model [9] with the only difference that this process already involves three waves (the pump wave, the first and second Stokes components of the SRS) and the pump depletion process is limited by the onset of generation of second Stokes component.

Since the first and second Stokes components are close to single-mode ones, to describe the evolution of their powers, a balance model of single-mode fibre SRS lasers can be used. This model works well both in the case of the RFL scheme (linear resonators of FBG pairs for first and second component of SRS) [13] and in the case of a half-open resonator with Rayleigh distributed feedback [14]. For a single-mode RFL [13], upon reaching the generation threshold of the second Stokes component, the generation power of the first Stokes component is saturated. The power of the transmitted pump radiation increases to compensate for the power lost by the first Stokes component to be converted to the second component, which we see in our case for the RFL scheme (Fig. 2). For a single-mode RRFL [14], with an increase in the power of the second Stokes component, the first Stokes component at the output should be depleted almost to zero. However, this depletion is limited by the early achievement of the generation threshold of the third order Stokes component, which is probably due to the injection of radiation at $\lambda = 1065$ nm from LD [6]. If such injection was absent (in particular, for a multimode SRS laser with diode pumping at $\lambda = 915$ nm [5]) and the generation threshold for the third Stokes component was not reached, the power of the first Stokes component at the output decreased to almost zero, when the power of the second Stokes component became maximum (27 W) [5].

The developed sources can be used for biomedical diagnostics in the wavelength range less than 1 μm, frequency doubling and quadrupling, for micromachining materials, in laser displays, etc.

Acknowledgements. This work was supported by the Russian Science Foundation (Grant No. 21-72-30024).

References

1. Babin S.A., Zlobina E.A., Kablukov S.I. *J. Sel. Top. Quantum Electron.*, **24** (3), 1400310 (2018).

2. Glick Y., Shamir Y., Sintov Y., Goldring S., Pearl S. *Opt. Fiber Technol.*, **52**, 101955 (2019).
3. Richardson D.J., Nilsson J., Clarkson W.A. *J. Opt. Soc. Am. B*, **27** (11), B63 (2010).
4. Kuznetsov A.G., Kablukov S.I., Wolf A.A., Nemov I.N., Tyrtyshnyy V.A., Myasnikov D.V., Babin S.A. *Laser Phys. Lett.*, **16** (10), 105102 (2019).
5. Evmenova E.A. et al. *Sci. Rep.*, **8** (1), 17495 (2018).
6. Kuznetsov A.G., Nemov I.N., Wolf A.A., Kablukov S.I., Babin S.A. *Opt. Express*, **29** (11), 17573 (2021).
7. Baek S.H., Roh W. *Opt. Lett.*, **29** (2), 153 (2004).
8. Terry N.B., Alley T.G., Russell T.H. *Opt. Express*, **15** (26), 17509 (2007).
9. Kuznetsov A.G., Kablukov S.I., Podivilov E.V., Babin S.A. *Quantum Electron.*, **50** (12), 1091 (2020) [*Kvantovaya Elektron.*, **50** (12), 1091 (2020)].
10. Abdullina S.R., Vlasov A.A., Babin S.A. *Quantum Electron.*, **40** (3), 259 (2010) [*Kvantovaya Elektron.*, **40** (3), 259 (2010)].
11. Wolf A.A., Dostovalov A.V., Vabnits S., Babin S.A. *Quantum Electron.*, **48** (12), 1128 (2018) [*Kvantovaya Elektron.*, **48** (12), 1128 (2018)].
12. Podivilov E.V., Kharenko D.S., Gonta V.A., Krupa K., Sidelnikov O.S., Turitsyn S., Fedoruk M.P., Babin S.A., Wabnitz S. *Phys. Rev. Lett.*, **122** (10), 103902 (2019).
13. Babin S.A., Churkin D.V., Podivilov E.V. *Opt. Commun.*, **226** (1–6), 329 (2003).
14. Babin S.A., Zlobina E.A., Kablukov S.I., Podivilov E.V. *Sci. Rep.*, **6**, 22625 (2016).